bioRxiv preprint doi: https://doi.org/10.1101/2025.05.26.656186; this version posted May 29, 2025. The copyright holder for this preprint (which was not certified by peer review) is the author/funder, who has granted bioRxiv a license to display the preprint in perpetuity. It is made available under a CC-BY 4.0 International license.

Synthesis of C8-vinyl chlorophylls *d* and *f* impairs far-red light photoacclimation and growth under far-red light

Afeefa K. CHAUDHARY[1], Lorenz K. FUCHS[1], Krzysztof PAWLAK[2], Gregory F. DYKES[3], Royston GOODACRE[1], Dennis J. NÜRNBERG[4,5], Daniel P CANNIFFE[1]*

[1]Department of Biochemistry, Cell & Systems Biology; Institute of Systems, Molecular & Integrative Biology, University of Liverpool, UK

[2]Materials Innovation Factory, University of Liverpool, UK

[3]Biomedical Electron Microscopy Unit, University of Liverpool, UK

[4]Institute of Experimental Physics, Freie Universität Berlin, Germany

[5]Dahlem Centre of Plant Sciences, Freie Universität Berlin, Germany

*d.canniffe@liverpool.ac.uk, +44 (0)151 795 7733

bioRxiv preprint doi: https://doi.org/10.1101/2025.05.26.656186; this version posted May 29, 2025. The copyright holder for this preprint (which was not certified by peer review) is the author/funder, who has granted bioRxiv a license to display the preprint in perpetuity. It is made available under a CC-BY 4.0 International license.

ABSTRACT

The inducible biosynthesis of chlorophylls *d* and *f* enables a subset of specialised cyanobacteria to perform oxygenic photosynthesis under far-red light—in the absence of visible wavelengths—via a process termed far-red light photoacclimation. These pigments, like the more common chlorophylls *a* and *b*, typically carry an ethyl substituent at the C8 position of the macrocycle, formed by reduction of a vinyl group by an 8-vinyl reductase enzyme. Here, we disrupted the gene encoding BciB, an 8-vinyl reductase found in the majority of cyanobacteria, in *Chroococcidiopsis thermalis* PCC 7203, a model for the study of far-red light photoacclimation. Disruption of *bciB* results in the synthesis of 8-vinyl chlorophyll *a* when the cells are grown in white light; on switching to far-red light, synthesis of 8V-forms of chlorophylls *d* and *f*, which have not been detected in nature, are synthesised in this strain. The *bciB* mutant exhibits sensitivity to high irradiance under both light regimes. Pigment analysis and whole-cell absorption and fluorescence spectroscopy reveal decreased synthesis of far-red absorbing chlorophylls, reduced photosystem assembly and an impaired acclimation to far-red light, and transmission electron microscopy demonstrates altered thylakoid membrane morphology in the mutant when compared to the wild type. These results demonstrate the importance of 8-vinyl group reduction for acclimation to far-red light.

bioRxiv preprint doi: https://doi.org/10.1101/2025.05.26.656186; this version posted May 29, 2025. The copyright holder for this preprint (which was not certified by peer review) is the author/funder, who has granted bioRxiv a license to display the preprint in perpetuity. It is made available under a CC-BY 4.0 International license.

INTRODUCTION

Photosynthesis, the process by which sunlight is captured and converted into the chemical energy that supports life on Earth, is dependent on the chlorophyll (Chl) family of pigments. These Chls act as antenna chromophores to capture photons and transfer derived excitation energy towards the photochemical reaction centre, where they are also involved in charge separation and the primary steps of photosynthetic electron transport [1]. Chl *a* is the ubiquitous pigment essential for oxygenic photosynthesis and is the sole Chl found in the majority of cyanobacteria. In addition to Chl *a*, plants, algae, and a few cyanobacteria in the Prochlorococcaceae, Prochlorotrichaceae (together formerly known as Prochlorales or prochlorophyta) and a single member of the Acaryochloridaceae synthesize Chl *b* [2,3], which carries a formyl group at C7 (**Fig. 1**), enhancing light capture in the blue and orange regions of the solar spectrum [4]. In 1993, a cyanobacterium was isolated from a colonial sea squirt off the coast of Palau that was found to contain Chl *d*, carrying a formyl group at C3 (see **Fig. 1**), as its major photopigment [5]. Chl *d* has a red-shifted absorption maximum compared to that of Chl *a*, displaying a Q_y band at 696 nm—31 nm longer than that of Chl *a*—and the high Chl *d*:Chl *a* ratio *in vivo* (>90% Chl *d*) accounts for the strongly red shifted absorption profile of this organism, *Acaryochloris marina*, relative to the majority of cyanobacteria, allowing it to capture light at wavelengths > 700 nm in the solar spectrum (far-red light; FRL) [5]. In 2010, another novel pigment, Chl *f*, carrying a formyl group at C2 resulting in a Q_y absorption maximum at 705 nm (see **Fig. 1**), was identified in a stromatolite from Shark Bay, Australia [6]. This pigment was accumulated by a cyanobacterium, *Halomicronema hongdechloris*, enriched by growth under FRL—conditions that mirror its ecological niche in the stromatolite—but Chl *f* in this cyanobacterium was found to be a minor component, making up 10% of the total Chl when grown under FRL, and undetectable in white light (400–700 nm; WL) [6,7]. Subsequently, this induction of the synthesis of Chl *f* upon growth in FRL was discovered in another cyanobacterium, *Leptolyngbya* sp. JSC-1, isolated from a floating microbial mat at 45°C close to La Duke Hot Spring, Montana, USA [8]. In this case it was discovered that Chl *f* synthesis occurred concomitant with synthesis of Chl *d* and the replacement of the core subunits of photosystems I (PSI), II (PSII), and the phycobilisome antenna with paralogous proteins encoded in a gene cluster, expression of which is controlled by a red/far-red phytochrome and two response regulators [8]. This response to growth in FRL, termed 'far-red light photoacclimation' (FaRLiP), results in the increase in expression by more than two times for ~900 genes, and a decrease to less than half for ~2000 genes, accounting for a two-fold change in expression of >40% of the genome [8]. Soon after, the ability to perform FaRLiP was discovered in morphologically diverse cyanobacteria, the majority from terrestrial environments in which competition for WL is fierce (e.g. microbial mats) or where FRL is enriched due to scattering of sunlight (e.g. soils) [9]; In these diverse organisms the FaRLiP response is dependent on a conserved cluster of 19 core genes (although some clusters contain a greater number) [10]. Each FaRLiP cluster contains two paralogs of the PSII core subunit gene *psbA*, one of which encodes a light-dependent enzyme for the synthesis of Chl *f* [11,12].

bioRxiv preprint doi: https://doi.org/10.1101/2025.05.26.656186; this version posted May 29, 2025. The copyright holder for this preprint (which was not certified by peer review) is the author/funder, who has granted bioRxiv a license to display the preprint in perpetuity. It is made available under a CC-BY 4.0 International license.

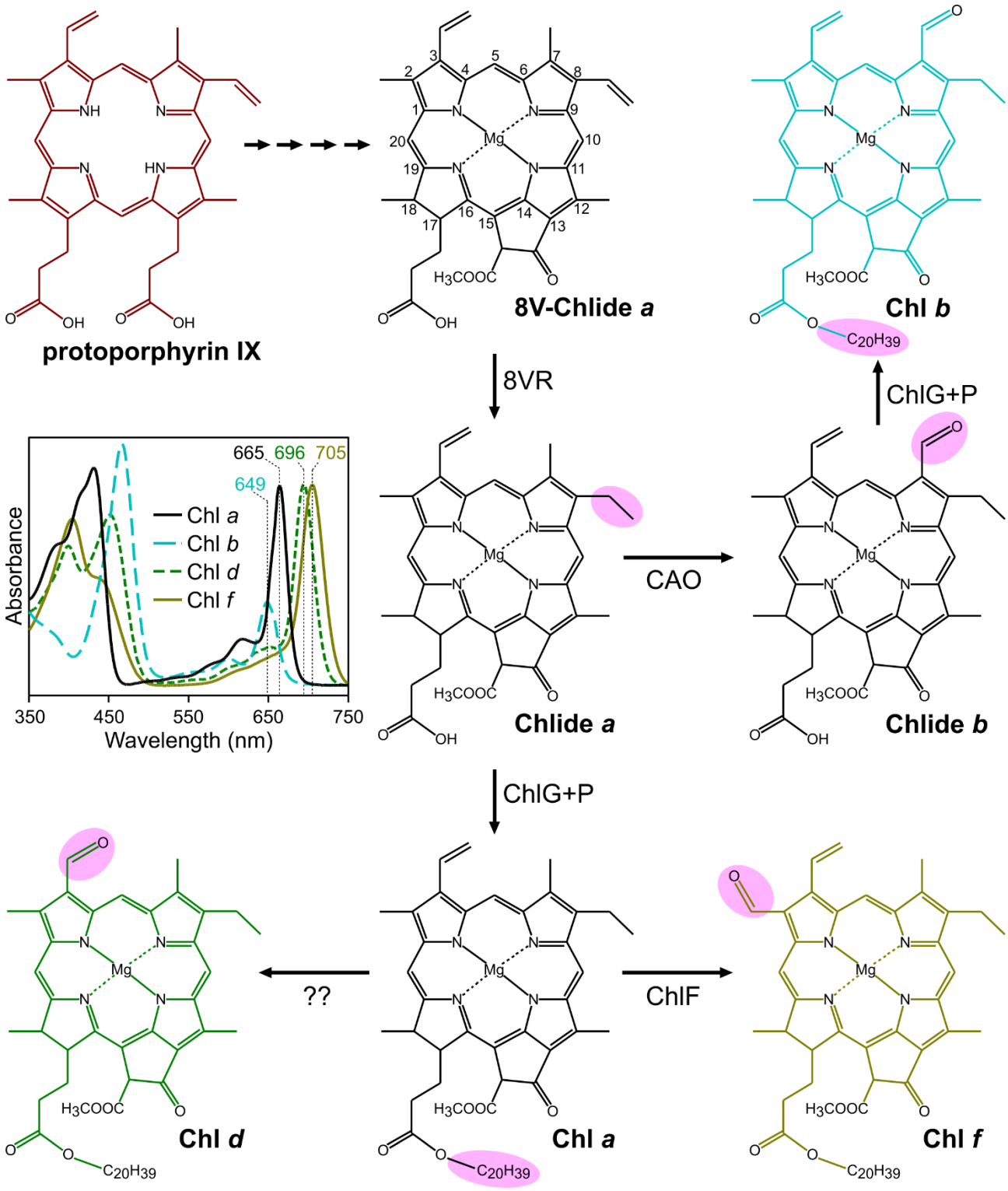


Figure 1. Terminal steps in the synthesis of Chls of oxygenic phototrophs. Protoporphyrin IX stands at the branchpoint between heme and Chl biosynthesis. IUPAC numbering of macrocycle carbons is displayed on 8V-Chlide, the universal precursor to all Chls. The routes to the synthesis of mature Chls are shown. The groups modified at each step are highlighted in pink, and the enzyme responsible is labelled at reaction arrows, except for Chl *d* synthase, which is currently unknown. CAO, chlorophyllide *a* oxygenase. 8VR, 8-vinyl reductase. ChlF, chlorophyll *f* synthase. ChlG, chlorophyll synthase. ChlP, geranylgeranyl reductase. Inset, absorption spectra of Chls are displayed, and their Q_y absorption maxima in methanol are labelled.

bioRxiv preprint doi: https://doi.org/10.1101/2025.05.26.656186; this version posted May 29, 2025. The copyright holder for this preprint (which was not certified by peer review) is the author/funder, who has granted bioRxiv a license to display the preprint in perpetuity. It is made available under a CC-BY 4.0 International license.

The mature pigments discussed above carry an ethyl group at the C8 position (8E), resulting from the reduction of a vinyl group on 8-vinyl (8V) chlorophyllide (Chlide) by an 8-vinyl reductase (8VR) enzyme (see **Fig. 1**); the only known exception to this are the marine *Prochlorococcus* spp. that naturally produce 8V-Chls *a* and *b* (also known as divinyl (DV)-Chl *a* and *b*) [13]. Outside of this special case, two unrelated classes of 8VR involved in the biosynthesis of chlorophylls are known to exist, BciA and BciB. BciA (EC 1.3.1.75) was first identified by screening mutants of *Arabidopsis thaliana*; mutations in the AT5G18660 locus led to the accumulation of 8V- rather than 8E-Chls *a* and *b* [14,15], and the recombinant enzyme produced in *Escherichia coli* was shown to reduce 8V-Chlide to 8E-Chlide [14]. Subsequently, BciA activities were demonstrated for proteins from rice [16], maize and cucumber [17], as well as in bacteriochlorophyll (BChl) *a*-synthesizing anoxygenic phototrophs including the green sulfur bacterium *Chlorobaculum tepidum* [18], and the purple phototrophic bacterium *Rhodobacter sphaeroides* [19]. *In vitro* assays performed with BciA-type 8VRs from various species have demonstrated that NADPH is the electron donor for this enzyme [16–18,20].

Despite also utilizing 8E-Chls, the genomes of most cyanobacteria do not contain orthologs of *bciA*, which indicated the existence of a second, unrelated 8VR. Two studies on the model cyanobacterium *Synechocystis* sp. PCC 6803 (*Synechocystis*) demonstrated that mutants in open reading frame (ORF) slr1923 were unable to grow under moderate light intensity and accumulated 8V-Chl *a* [21,22]. Subsequently, an ortholog of slr1923 from the green sulfur bacterium *Chloroherpeton thalassium* was shown to complement a *bciA* mutant of *Chlorobaculum tepidum*, recovering synthesis of 8E-(B)Chls and confirming the activity of the second class of 8VRs, annotated as BciB (EC 1.3.7.13) [23]. A study on the *in vitro* activity of the BciB-type 8VR from *Chloroherpeton thalassium* showed that the enzyme is a flavin adenine dinucleotide (FAD)-containing [4Fe–4S] protein, deriving electrons from reduced ferredoxin [24].

8VR mutants in plants and cyanobacteria display disrupted thylakoid membrane development and light sensitivity [14,16,21]. 8V-Chls *d* and *f* have never been reported in nature, so the effect that synthesis of these pigments have on the utilization of FRL is unknown. Species of *A. marina* appear to be unique among cyanobacteria by employing both BciA and BciB to ensure production of Chl *d* with an 8E group [25]. In the present study we constructed a *bciB* mutant of the model FRL-absorbing cyanobacterium *Chroococcidiopsis thermalis* PCC 7203 (hereafter *C. thermalis*) to assess the effect of 8V-Chls *d* and *f* on the FaRLiP process and growth under wavelengths longer than 700 nm.

MATERIALS & METHODS

Growth of bacterial strains. *C. thermalis* was grown photoautotrophically in BG-11 medium [26] buffered with 10 mM 2-[(2-Hydroxy-1,1-bis(hydroxymethyl)ethyl)amino] ethanesulfonic acid (TES) pH 8.2. Cells were routinely grown and maintained on solid medium containing 1.5% (w/v) Bacto agar or in liquid under moderate light intensity (30 µmol photons·m^{-2}·s^{-1}) provided by white-light LEDs at 30°C; when required, high light was provided by the same LEDs at 250 µmol photons·m^{-2}·s^{-1}. FRL was provided by LEDs with emission

bioRxiv preprint doi: https://doi.org/10.1101/2025.05.26.656186; this version posted May 29, 2025. The copyright holder for this preprint (which was not certified by peer review) is the author/funder, who has granted bioRxiv a license to display the preprint in perpetuity. It is made available under a CC-BY 4.0 International license.

centred at 730 nm (Shenzhen Gouly LED Limited); moderate and high intensity FRL was calculated at equivalents of 20 and 75 µmol photons·m^{-2}·s^{-1}, respectively. Light intensity was measured with a LI-COR LI-250 radiometer equipped with a LI-190R pyranometer visible–near infrared sensor. When necessary, BG-11 medium was supplemented with 20 µg·ml^{-1} erythromycin.

E. coli strains were grown in lysogeny broth (LB) at 37°C in a rotary shaker at 250 rpm. When necessary, LB was supplemented with 30 µg·ml^{-1} spectinomycin, 100 µg·ml^{-1} ampicillin, and 12.5 µg·ml^{-1} chloramphenicol. All strains and plasmids used in this study are listed in Table S1.

Plate-based growth assays. Drop growth assays of *C. thermalis* strains were conducted using liquid cultures grown under moderate light, adjusted to OD_{780} = 0.4 after Dounce homogenisation, and serially diluted. Dilutions were spotted onto solid medium and incubated at moderate and high (250 µmol photons·m^{-2}·s^{-1}) light intensity.

Mutagenesis of *C. thermalis*. DNA sequences of ~2.5 kb flanking the targeted sites for insertion of an antibiotic resistance cassette were amplified from the genome of *C. thermalis* with relevant UpF and UpR/DownF and Down R primer pairs (see Table S2 for all primer sequences) and fused by overlap extension PCR, such that the flanking regions were separated by a sequence containing XhoI and AvrII restriction sites. These fragments were digested with EagI and SacI and cloned into similarly digested pRL277 [27]. The erythromycin resistance cassette from pRL692 [28] was amplified with EmRF and EmRR, digested with XhoI and AvrII, and ligated into the same sites introduced by the overlap extension step in the constructed pRL277 plasmids. These plasmids were sequenced and transformed into the *E. coli* donor strain HB101, prepared to contain conjugal and helper plasmids pRL443 [29] and pRL528 [30], respectively, for biparental mating. Resulting HB101 transformants were grown overnight; 20 ml of culture was pelleted by centrifugation at 3000 x *g*, and the pellet was gently resuspended in 10 ml sterile LB. This was repeated three times to remove all traces of antibiotics, and the cells were finally resuspended in 200 µl LB. Meanwhile, 30 ml of freshly grown *C. thermalis* for each mating was sonicated for 2 x 30 s at low power to disperse clumps of cells and centrifuged as above. The pellet was washed with 10 ml sterile BG-11 medium three times and finally resuspended in 200 µl BG-11. These cells were mixed with the 200 µl suspension of HB101 cells in LB and incubated in the dark at RT for 8 h, before being spotted onto a sterile Whatman mixed cellulose ester filter membrane (0.45 µm pore size) overlaid on a BG-11 agar plate lacking antibiotics, and incubated at 30°C under dim light (~2 µmol photons·m^{-2}·s^{-1}) for 24 h, after which time the membrane was transferred to a BG-11 plate containing erythromycin and exposed to moderate light. Green colonies appeared after ~5 weeks; these were patched onto fresh selective plates for screening by colony PCR using the relevant CheckF and CheckR primers, which bind outside the regions of homology used for recombination, and positive patches were serially streaked onto selective plates to isolate axenic colonies away from any remaining HB101 cells.

bioRxiv preprint doi: https://doi.org/10.1101/2025.05.26.656186; this version posted May 29, 2025. The copyright holder for this preprint (which was not certified by peer review) is the author/funder, who has granted bioRxiv a license to display the preprint in perpetuity. It is made available under a CC-BY 4.0 International license.

Absorption spectroscopy. UV/vis/near-IR absorption spectra of homogenised whole cells were collected on a Cary 3500 spectrophotometer (Agilent Technologies) scanning between 300 and 1100 nm at 1 nm intervals with a 0.1 s integration time.

Fluorescence spectroscopy. Cells were harvested from liquid medium and resuspended in BG-11 containing 60% (v/v) glycerol by gentle homogenisation. Cryogenic fluorescence emission spectra were measured at 77 K in an OptistatDN-X cryostat (Oxford Instruments) on an Edinburgh Instruments FLS1000 spectrofluorometer between 600 and 850 nm at 1 nm intervals and a 0.2 s dwell time, after excitation at 440 nm.

Extraction and analysis of pigments. Chls were extracted from cell pellets after washing in 20 mM HEPES pH 7.2 by adding 9 pellet volumes of 7:2 (v/v) acetone: methanol, vortex mixing for 30 s, and incubating on ice for 15 min. Extracts were clarified by centrifugation (15,000 × *g* for 5 min at 4°C), and the supernatants were filtered through 0.22 µm PVDF membrane filters and immediately analysed by high-performance liquid chromatography (HPLC) on an Agilent 1100 system. Chl species were separated on a Supelco Discovery HS C18 column (5 µm particle size, 120 Å pore size, 250 × 4.6 mm) using a program modified from that of a previously published method [31]. Solvents A and B were 80:20 (v/v) methanol:500 mM ammonium acetate and 80:20 (v/v) methanol:acetone, respectively. Pigments were eluted at 1 ml·min^{-1} at 40°C on a linear gradient of 92 to 94% solvent B over 25 min, increasing to 100% to wash the column. Elution of Chl species was monitored by checking absorbance at 665 nm (Chl *a*), 696 nm (Chl *d*), and 706 nm (Chl *f*).

Transmission electron microscopy. *C. thermalis* cells were prefixed with 2.5% (w/v) glutaraldehyde and 4% (w/v) paraformaldehyde in 0.1 M sodium cacodylate pH 7.2 and postfixed with 1% (w/v) osmium tetroxide, 1.5% (w/v) potassium ferrocyanide, 0.1% (w/v) thiocarbohydrazide, 2% (w/v) osmium tetroxide and 1% (w/v) uranyl acetate. Samples were dehydrated with increasing ethanol concentrations (30−100%), embedded in TAAB 812 premix resin, and cut into thin sections (70 nm). These were post-stained with 3% (w/v) lead citrate. Images were recorded using a Tecnai G2 Spirit BioTWIN transmission electron microscope (FEI) equipped with a Gatan Rio 16 camera.

RESULTS

Construction of *C. thermalis* mutants.

To test the effects of using 8V Chls for growth under WL and FRL, the *bciB* gene of *C. thermalis* (Chro_1099) was disrupted with an erythromycin resistance cassette, generating a Δ*bciB* mutant (**Fig. 2A, B**). To act as a control for experiments with the Δ*bciB* mutant, as well as other mutants to be constructed in the future in *C. thermalis*, an additional mutant was generated in which the erythromycin resistance cassette was

bioRxiv preprint doi: https://doi.org/10.1101/2025.05.26.656186; this version posted May 29, 2025. The copyright holder for this preprint (which was not certified by peer review) is the author/funder, who has granted bioRxiv a license to display the preprint in perpetuity. It is made available under a CC-BY 4.0 International license.

integrated into the genome between the converging Chro_1103 and Chro_1104 ORFs, ensuring that expression of these and neighbouring genes are not disrupted (**Fig. 2A, C**). This mutant, WT^{Em}, could then be used for direct comparison with Δ*bciB* when selection with antibiotic was necessary.

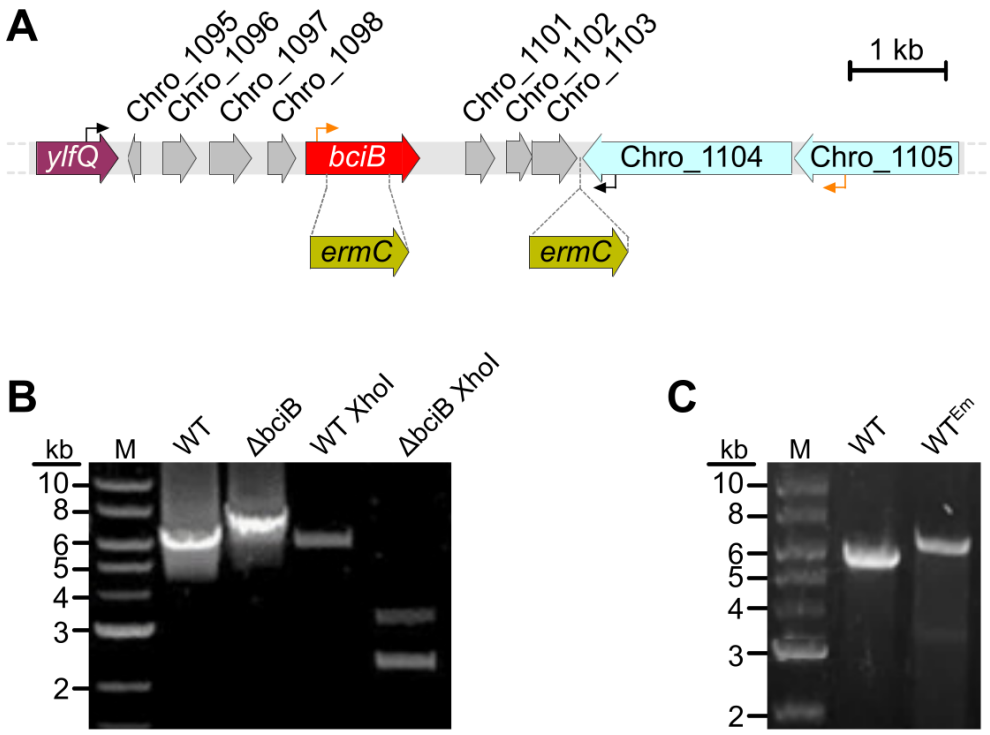


Figure 2. Construction of mutants of *C. thermalis*.
A. Cartoon representation of the genomic location of the *bciB* gene. Sites targeted for the erythromycin resistance cassette (*ermC*) to disrupt *bciB* or generate a neutral site integration are indicated by dashed lines, and primer binding sites used to screen these mutations are indicated by black and orange arrows, respectively. *B*. PCR confirming the disruption of *bciB* from isolated genomic DNA. The WT amplicon does not contain a XhoI restriction site, so only that generated from the *bciB* mutant results in two shorter fragments of DNA after digestion with this restriction enzyme. *C*. PCR confirming the neutral site integration of the erythromycin resistance cassette, generating the WT^{Em} mutant, from isolated genomic DNA.

Absorption profiles of *C. thermalis* strains.

The WT^{Em} and Δ*bciB* strains of *C. thermalis* were cultured in liquid medium and illuminated by moderate intensity WL, and absorption spectra of whole cells were measured (**Fig. 3**, dashed-line spectra). When standardised by cell number, the Δ*bciB* mutant displays reduced amplitude peaks corresponding to photosynthetic pigment–protein complexes, indicating their decreased assembly in these cells. The Δ*bciB* mutant displays 8 nm and 1 nm red-shifts in Soret and Q_y absorption bands of the Chl-containing complexes, respectively, when compared to WT^{Em}. When these strains were cultured moderate intensity FRL for 12 days, allowing sufficient time for them to have undergone the slow FaRLiP process, far-red absorbing features in the whole cell spectra were apparent (**Fig. 3**, solid-lined spectra, highlighted box). The absorption maxima

bioRxiv preprint doi: https://doi.org/10.1101/2025.05.26.656186; this version posted May 29, 2025. The copyright holder for this preprint (which was not certified by peer review) is the author/funder, who has granted bioRxiv a license to display the preprint in perpetuity. It is made available under a CC-BY 4.0 International license.

displayed by the WT^{Em} strain were consistent between growth under WL and FRL, but growth under FRL results in an increase in the ratio of Chl-containing complexes to phycobilisomes in this strain. In comparison to WT^{Em}, the Δ*bciB* mutant again displayed peaks associated with the photosystems and phycolbilisome antenna with reduced amplitude, including the far-red absorbing feature, and the mutant displayed a 7 nm red-shift in the Soret absorption band, but surprisingly also showed a Q_y band blue-shifted by 4 nm relative to WT^{Em}, and by 5 nm compared to its maximum when grown under white light. The mutant also displays a decrease in the ratio of Chl-containing complexes to phycobilisomes when grown under FRL compared to WL, the opposite effect that growth under FRL elicits on WT^{EM}.

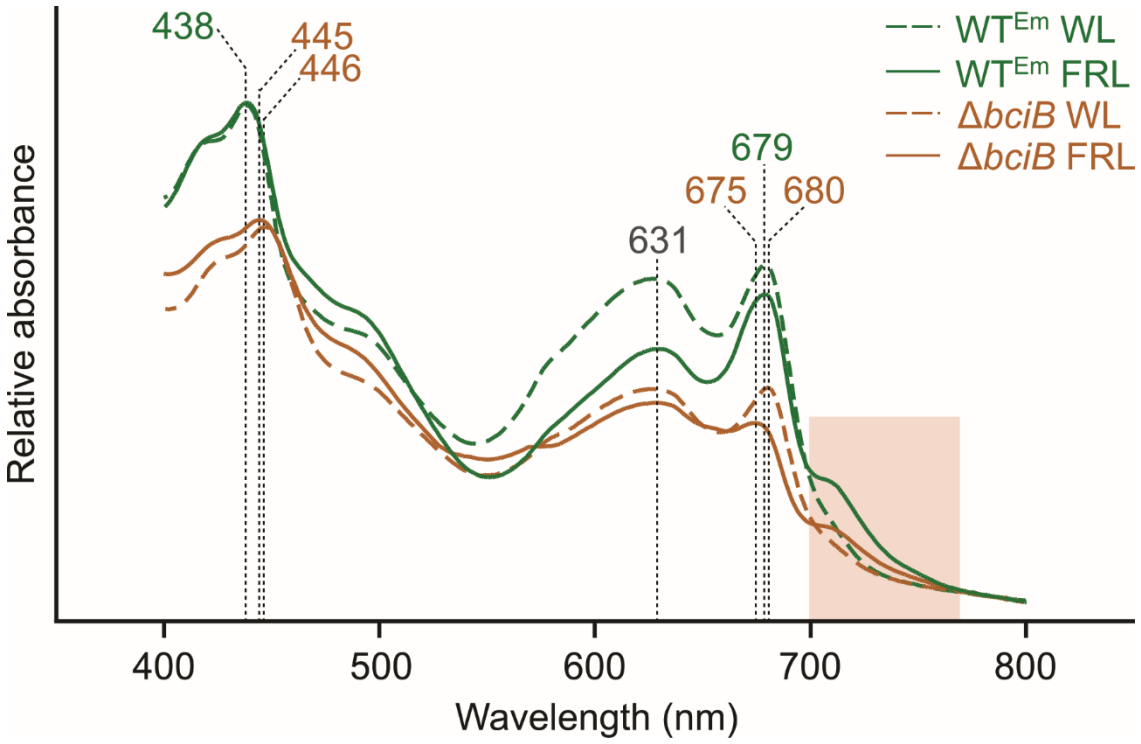


Figure 3. Whole cell absorption spectra of *C. thermalis* cells grown under WL and FRL. Cells from liquid cultures grown under moderate light were homogenised to break up clumps of cells, standardised by OD_{780}, and their absorption spectra recorded. Absorption maxima of pigment-containing complexes are indicated by dashed lines, and the region from 700–770 nm in which spectral features appear in FaRLiP-capable cyanobacteria is highlighted.

Pigment biosynthesis under white light and far-red light.

Pigments were extracted from liquid cultures of WT^{Em} and Δ*bciB* grown under both WL and FRL and subjected to analysis by reverse-phase HPLC (**Fig. 4**). When grown under WL, WT^{Em} produces Chl *a* (carrying the canonical 8E group), while Δ*bciB* accumulates 8V-Chl *a*, identifiable by its shorter retention time and red-shifted Soret maximum in its absorption spectrum. Under FRL, WT^{Em} synthesises Chls *f* and *d* in addition to Chl *a*. The Δ*bciB* mutant also accumulates two additional pigments, each with a shorter retention time than their equivalent extracted from WT^{Em}. The absorption spectra of these peaks demonstrate red-shifted Soret maxima, and in the case of the Chl *f* species, a blue-shifted Q_y maximum to 703 nm from 706 nm. These

bioRxiv preprint doi: https://doi.org/10.1101/2025.05.26.656186; this version posted May 29, 2025. The copyright holder for this preprint (which was not certified by peer review) is the author/funder, who has granted bioRxiv a license to display the preprint in perpetuity. It is made available under a CC-BY 4.0 International license.

characteristics allow us to assign these pigments as 8V-Chls *d* and *f*, which have not been found in nature, to date. The spectrum of 8V-Chl *d* contains peaks at 439 and 665 nm, contributed from a minor Chl *a*-type species (perhaps esterified with a C15 tail); these pigments could not be separated to deconvolute their individual spectra despite employing a range of methods and columns. Chl *f* makes up ~10% of the total Chls in WT^{Em} grown under FRL, consistent with other studies on FaRLiP cyanobacteria [32,33]. This contribution is reduced to ~3% of total Chls in the Δ*bciB* mutant, indicating that the FaRLiP response is impaired when 8V-Chls are synthesised.

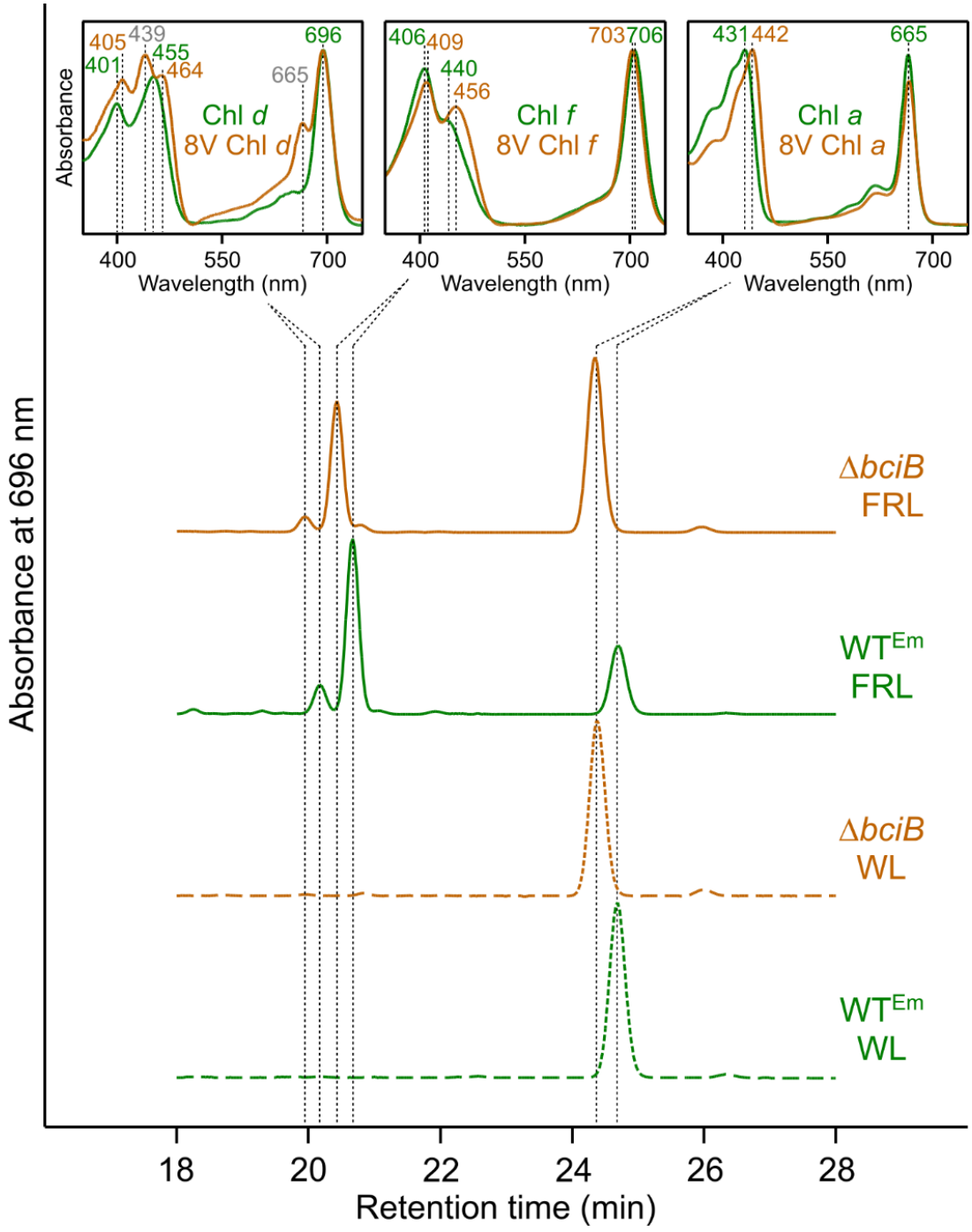


Figure 4. HPLC analysis of pigments extracted from described strains of *C. thermalis*. Pigments were extracted from liquid cultures grown in moderate intensity WL (dashed traces) and

bioRxiv preprint doi: https://doi.org/10.1101/2025.05.26.656186; this version posted May 29, 2025. The copyright holder for this preprint (which was not certified by peer review) is the author/funder, who has granted bioRxiv a license to display the preprint in perpetuity. It is made available under a CC-BY 4.0 International license.

FRL (solid traces). In-line absorption spectra of peaks are shown in the inset panels, with absorption maxima used to identify the pigment species. Traces are normalised to major peak height for clarity.

Energy transfer in whole cells.

Whole-cell fluorescence emission spectra at 77 K were recorded for both strains (**Fig. 5**). When Chls were excited at 440 nm, WL grown cells display a major emission maximum at 726 nm and a broad, long-wavelength emission band at ~800 nm, thought to derive from excitonically-coupled Chls at the monomer interface of dimeric and tetrameric PSI, which predominate in WL grown *C. thermalis* [34] (**Fig. 5A**). The Δ*bciB* strain displays prominent emission features with maxima at 641 nm, 666 nm, and 685 nm, the first two of these likely derived from phycocyanin and allophycocyanin, respectively, and the last from PSII. The features associated with allophycocyanin and PSII are detectable in the WT^{Em} spectrum, but are much less apparent. However, a conserved feature emitting at 695 nm, which has been associated with PSII [35], is more pronounced in WT^{Em} than in the Δ*bciB* cells.

When cells grown under FRL were excited at 440 nm, the major emission peak in WT^{Em} is shifted to 752 nm, derived from FRL-PSI, with a prominent shoulder associated with FRL-PSII at 740 nm (**Fig. 5B**). The equivalents in the Δ*bciB* mutant are blue-shifted by 4 nm and 7 nm, respectively. A similar blue-shift is observed for the PSI associated emission above 800 nm. The peak at 813 nm in WT^{Em} is shifted to 809 nm in the Δ*bciB* mutant. The emission band at 686 nm associated with WL-PSII is also still apparent in the Δ*bciB* mutant, which may be indicative of impaired and/or incomplete acclimation to FRL.

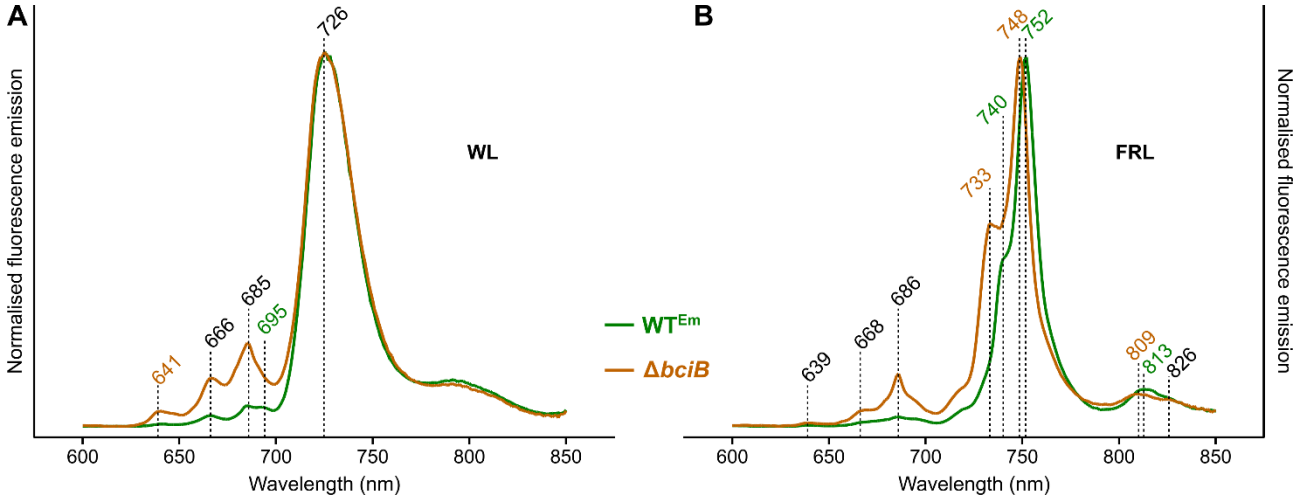


Figure 5. Low-temperature fluorescence emission spectra of *C. thermalis* cells grown under WL and FRL. Fluorescence emission spectra of WT^{Em} (green) and Δ*bciB* (orange) cells at 77 K, excited at 440 nm. **A**, Cells grown in WL. **B**, Cells grown in FRL. The emission intensities are normalised to those of PSI maxima, and emission features present in both strains, WT^{Em} only, and Δ*bciB* only are indicated in black, green, and orange, respectively.

bioRxiv preprint doi: https://doi.org/10.1101/2025.05.26.656186; this version posted May 29, 2025. The copyright holder for this preprint (which was not certified by peer review) is the author/funder, who has granted bioRxiv a license to display the preprint in perpetuity. It is made available under a CC-BY 4.0 International license.

Testing the light-sensitivity of *C. thermalis*.

8VR mutants of *Synechocystis* and *A. thaliana* are sensitive to high-intensity WL [14,21]. Due to aseriate (clumping) morphology of *C. thermalis*, drop growth assays on solid medium were conducted to determine if the same effect is observed with this cyanobacterium, rather than monitoring absorbance of liquid cultures (**Fig. 6**). Under moderate light conditions, both WT^{Em} and Δ*bciB* perform equally well, indicating that production of 8V-Chl *a* does not impart sensitivity at this light intensity. However, at 250 µmol photons·m^{-2}·s^{-1}, Δ*bciB* cells are completely bleached, while the WT is able to grow, albeit inhibited when compared to the moderate light regime.

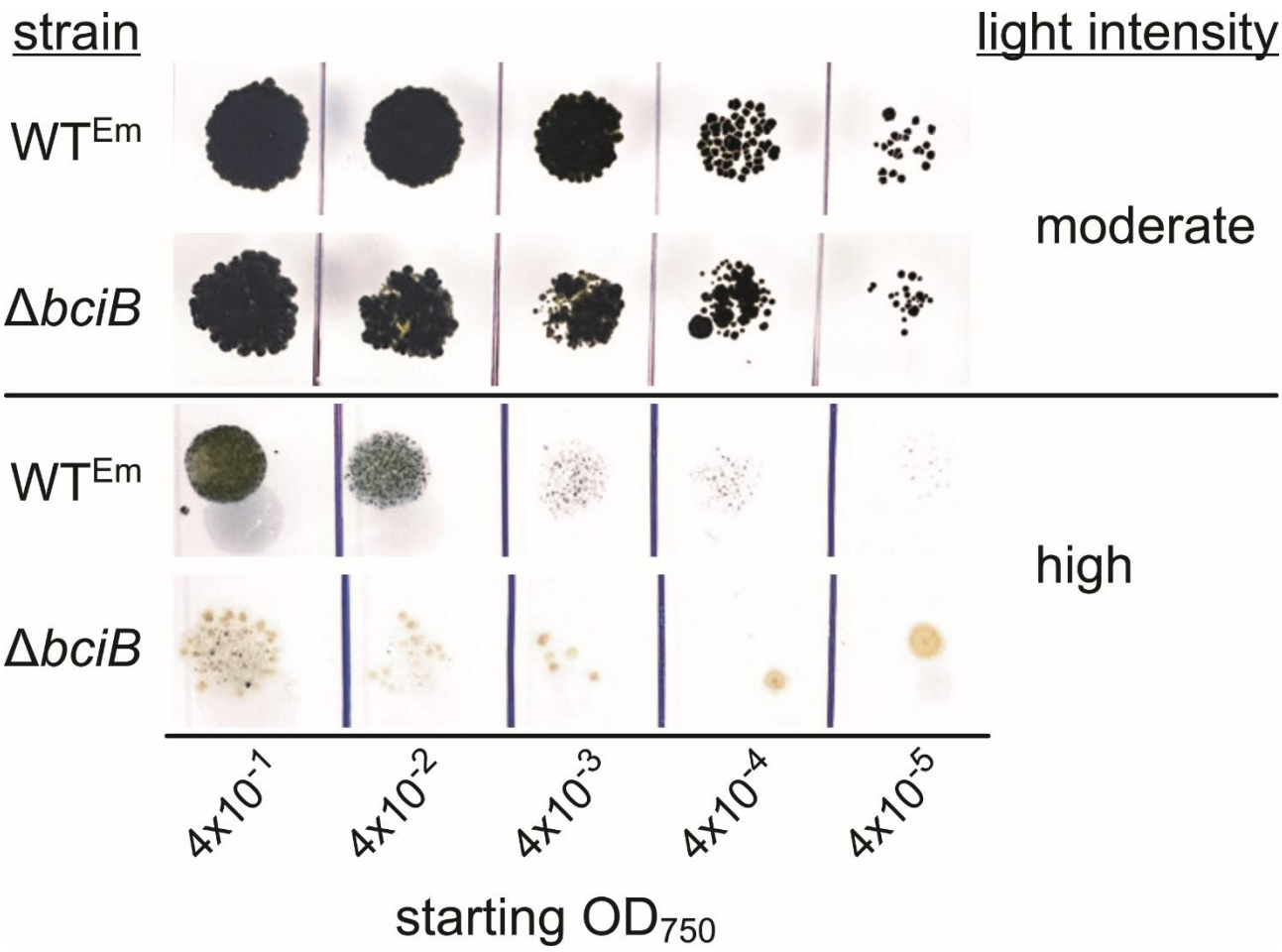


Figure 6. Drop growth assays of *C. thermalis* at moderate and high intensity WL. Clumps of cells from liquid cultures grown at moderate light were manually dispersed in a Dounce homogeniser, standardised by OD_{750} and serially diluted before spotting onto solidified BG-11 agar.

Light sensitivity under FRL was also tested. Since growth under this condition is too slow to be performed on plates, mid-exponential phase cells cultured under moderate WL were transferred to moderate and high FRL and allowed to undergo FaRLiP. Under moderate FRL conditions, those used to obtain the absorption spectra in Fig. 3, liquid cultures of WT^{Em} and Δ*bciB* are green, with no clear signs of bleaching (**Fig. 7**). However, when cultures are transferred to high intensity FRL to undergo FaRLiP, the Δ*bciB* cells bleach completely, and cannot be recovered when transferred back to moderate intensity WL (not shown). These results indicate

bioRxiv preprint doi: https://doi.org/10.1101/2025.05.26.656186; this version posted May 29, 2025. The copyright holder for this preprint (which was not certified by peer review) is the author/funder, who has granted bioRxiv a license to display the preprint in perpetuity. It is made available under a CC-BY 4.0 International license.

that a similar sensitivity to high intensity illumination is displayed by *C. thermalis* cells under WL and FRL conditions when 8V Chls are synthesised.

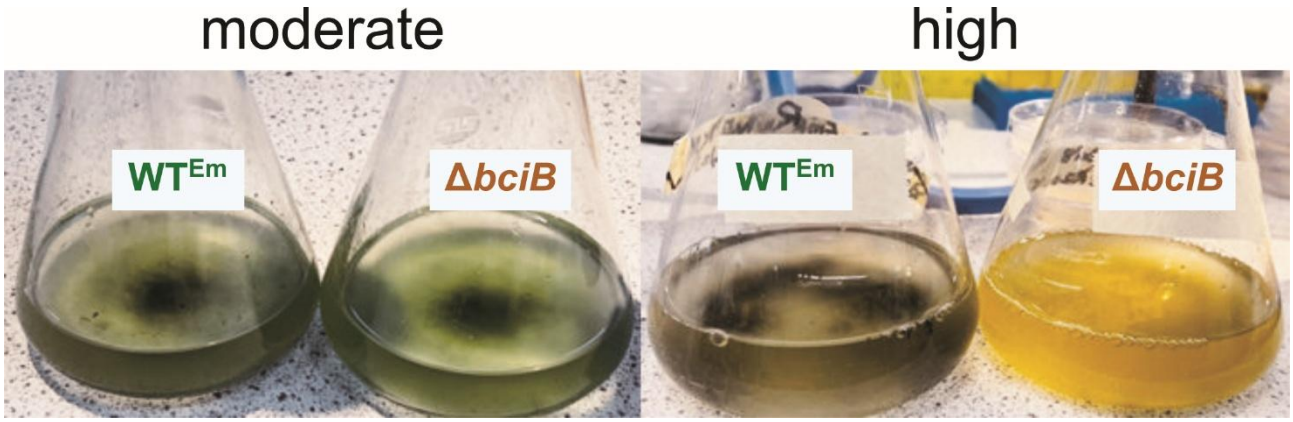


Figure 7. Liquid cultures of *C. thermalis* grown under moderate and high intensity FRL. Photographs were taken after 12 days of incubation under the relevant condition to allow the FaRLiP process to take place.

Analysis of membrane ultrastructure.

To determine if membrane morphology is affected by the synthesis of 8V-Chls, transmission electron micrographs of thin sections of *C. thermalis* cells were taken (**Fig. 8**). Cells were cultured under moderate intensity WL or FRL to mid exponential phase to provide moderate light samples. To generate samples exposed to high intensity light, additional mid exponential phase cells grown under moderate light were shifted to high intensity light for 2 days, allowing for bleaching effects to be observed while limiting cell death. WT^{Em} cells display a curved thylakoid membrane morphology under each condition, with overall cellular membrane density decreasing as light intensity increases under both WL and FRL conditions. This reduction in overall membrane density is also displayed by the Δ*bciB* mutant as light intensity increases, but this is accompanied by fragmentation of the thylakoids at high light, with uninterrupted membranes spanning the entire cell missing in these cells. The curvature of membranes in the Δ*bciB* mutant is also different to that of WT^{Em}; cells synthesising 8E-Chls display thylakoids that bend into the cytoplasm, increasing overall surface area, while those in the mutant synthesising 8V-Chls remain contiguous with the cytoplasmic membrane.

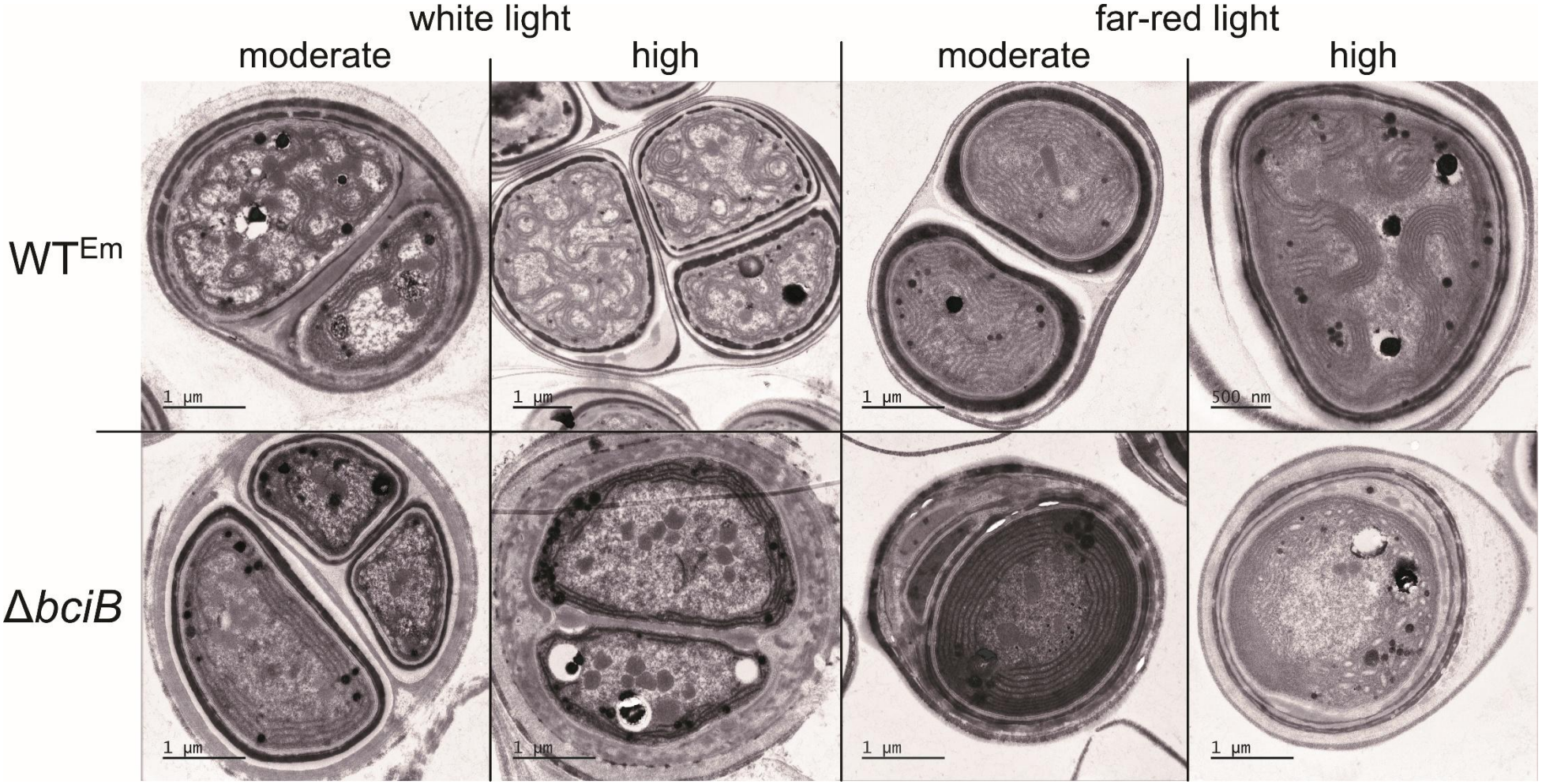


Figure 8. Transmission electron micrographs of thin sections of *C. thermalis* cells, grown under moderate and high WL and FRL. Electron microscopic images from WT^{Em} cells (upper panels) and Δ*bciB* cells (lower panels).

bioRxiv preprint doi: https://doi.org/10.1101/2025.05.26.656186; this version posted May 29, 2025. The copyright holder for this preprint (which was not certified by peer review) is the author/funder, who has granted bioRxiv a license to display the preprint in perpetuity. It is made available under a CC-BY 4.0 International license.

DISCUSSION

In the present study we have determined that the synthesis of 8V-Chls results in light sensitivity under both WL and FRL in the model FaRLiP cyanobacterium *C. thermalis*. The results under WL mirror those reported for mutants of *Synechocystis* and *A. thaliana* accumulating 8V-Chls [21,14], but we report the first analysis of growth using 8V Chls *d* and *f* under FRL. Our results indicate that FaRLiP is impaired in the *bciB* mutant, with a much less prominent FRL-absorbing feature present in the whole-cell absorption spectrum, and a concomitant reduction in the Chl *f*:Chl *a* ratio, than is found in WT^{Em} cells.

Under both WL and FRL conditions, the *bciB* mutant accumulates fewer Chl-containing photosystems than WT^{Em}, as indicated by the whole-cell absorption spectra. Similarly, under each condition tested, the *bciB* mutant displays an altered membrane morphology, where the characteristic bending thylakoids that curve into the centre of the cell, found in unmodified cells under both WL and FRL, are lost [34]. This lack of bending results in a reduction in the overall surface area of membrane in which to house PSII and PSI, and accounts for the loss in amplitude of the Chl-complex associated feature in the absorption spectra, but the direct cause of this change in morphology is not immediately obvious. The change in membrane shape is somewhat reminiscent of the effect of deletion of *curT* in *Synechocystis* [36]; the protein encoded by this gene is involved in thylakoid curvature in plants and cyanobacteria [37]. The genome of *C. thermalis* contains three orthologs of *curT*, which may in some part account for the extreme curvature of the membranes in this organism. However, further work is required to directly link synthesis of 8V-Chls to membrane morphology in the *bciB* mutant, including the fragmentation of these membranes under high-light conditions.

The high-intensity FRL employed in the current study may not be biologically relevant for certain environments where FaRLiP cyanobacteria are found (e.g. stromatolite, caves, microbial mats), where irradiance never reaches levels tested herein. However, high-intensity FRL may be experienced by cells growing under the surface layer of salt flats, where WL is almost completely reflected and FRL transmits, and under the canopy of plants, where FR wavelengths make up more than half of incident photons between 400–700 nm [38]. *Chroococcidiopsis* spp. are often found in hot desert environments, where photon flux can be extremely high [39]. It may be that FaRLiP cyanobacteria adapted to low-irradiance environments may better tolerate synthesis of 8V-Chls under these conditions.

It is notable that the clumping morphology of *C. thermalis* is less pronounced when cultured under FRL than under WL, which may permit a greater number of cells in a colony to access FRL. Under full spectrum sunlight, clumped colonies of FaRLiP-capable cyanobacteria may contain both cells performing canonical WL phototrophy and others that are limited to using FRL. It has been reported that *Chlorogloeopsis fritschii* PCC 6912, a FaRLiP cyanobacterium that also has a clumping morphology, produces Chls *d* and *f* when cultured in natural sunlight, but not when cultured under WL [40]. This is probably an effect of self-shading by the outer cells of the clump, and FRL being enriched as it penetrates the colony. If the common morphology of

bioRxiv preprint doi: https://doi.org/10.1101/2025.05.26.656186; this version posted May 29, 2025. The copyright holder for this preprint (which was not certified by peer review) is the author/funder, who has granted bioRxiv a license to display the preprint in perpetuity. It is made available under a CC-BY 4.0 International license.

C. thermalis was retained under FRL, a similar scenario would occur, with the outer cells of clumps harvesting photons in the 700–780 nm range and restricting light availability to cells in the centre; a switch to a more planktonic morphology allows a greater number of cells to access FRL, but which may come at a cost of easier predation or loss of particulate organic carbon from the centre of the clump [41]. Interestingly, this is in contrast to the behaviour of *Acaryochloris marina*, which switches from a planktonic state when grown under WL to forming biofilms when cultured under FRL, although pigment biosynthesis in this organism is not altered during this switch [42].

Prochlorococcus, thought to be the most abundant genus on Earth, use 8V Chls *a* and *b*, naturally lacking 8VR enzymes. Many *Prochlorococcus* spp. are found in surface water, where photon flux can reach very high intensities [43]. It has been proposed that methionine 205 and cysteine 282 residues in the D1 (PsbA subunit of the PSII reaction centre (numbered according to *Thermosynechococcus vestitus* BP-1)—conserved in the *Prochlorococcus* D1, where valine and glycine are conserved, respectively, in 8E-Chl *a* cyanobacteria—play a role in the ability of these organisms to tolerate high light [44]. A *Synechocystis* mutant synthesising 8V-Chl *a*, modified to carry these *Prochlorococcus* residues gained light tolerance in an additive manner with V205M followed by G282C substitutions [44]. Interestingly, the C282 residue is found in the D1 subunit of Chl *d*-synthesising *Acaryochloris marina* strains, and is also found in the FRL-D1 protein produced when FaRLiP cyanobacteria are cultured under FRL (Figure S1). A structural alignment of the D1 subunits of WL-utilising *Synechocystis* [45] and of the FRL-PSII used by *Synechococcus* sp. PCC 7335 [46], along with Alphafold models of FRL-D1 from *C. thermalis* and D1 from the type strain of *Prochlorococccus* (*P. marinus* MIT 9313) [47] are shown in **Fig. 9**. The residues in these positions are in close proximity to the P_{D1}–P_{D2} special pair and $Pheo_{D1}$ pigments involved in photosynthetic electron transfer, but do not directly coordinate these cofactors. It could be that the bulkier methionine in place of valine at position 205 in the *Prochlorococcus* subunit reduces a steric clash between a less flexible 8V group and the protein backbone, or could play a role in limiting photodamage, as suggested by Ito and Tanaka [44]. A target of future work will be to make the V205M mutation in the FRL-D1-encoding *psbA3* gene in Δ*bciB* and WT^{Em} strains of *C. thermalis* to determine if enhanced tolerance to high intensity FRL can be conferred when using 8V-Chls, and what the penalties of the mutation are when using 8E-Chls, respectively.

bioRxiv preprint doi: https://doi.org/10.1101/2025.05.26.656186; this version posted May 29, 2025. The copyright holder for this preprint (which was not certified by peer review) is the author/funder, who has granted bioRxiv a license to display the preprint in perpetuity. It is made available under a CC-BY 4.0 International license.

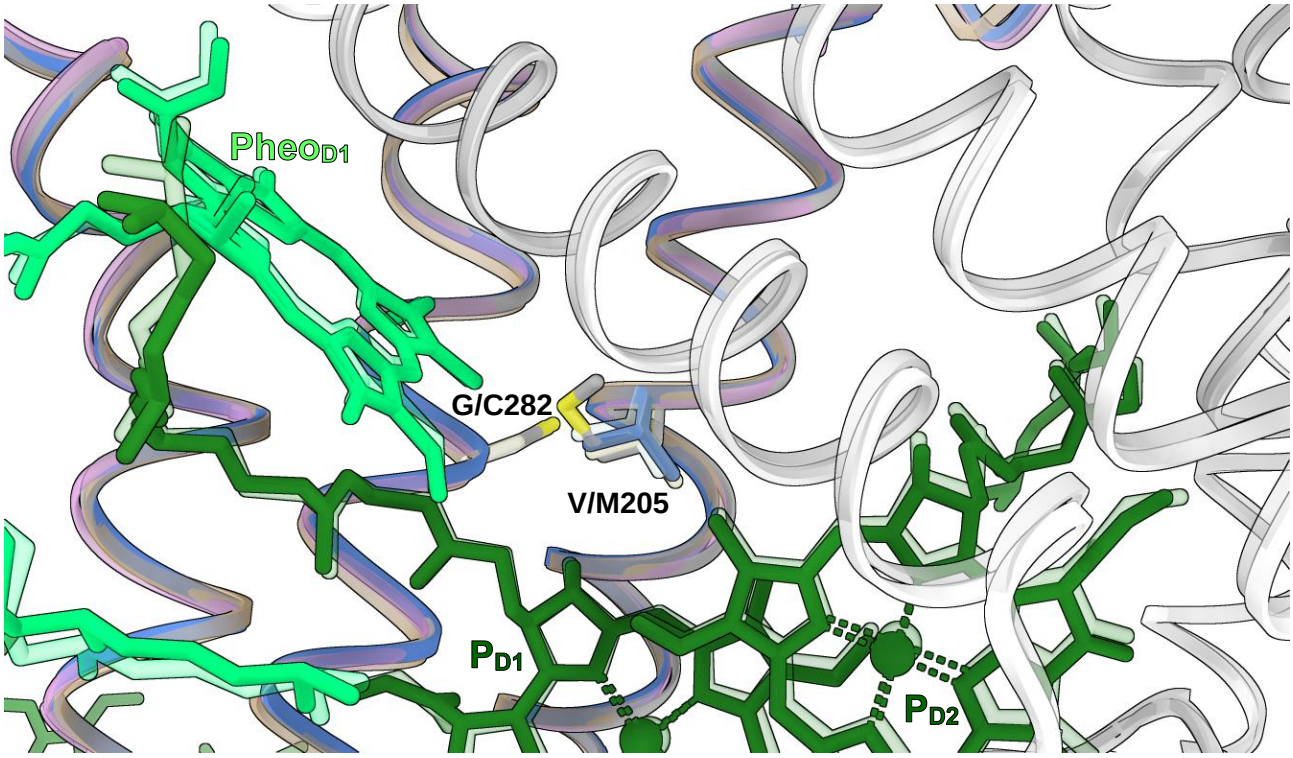


Figure 9. Structural alignment of D1 proteins. WL D1 of *Synechocystis* sp. PCC 6803 (7N8O; cornflower blue), FRL-D1 from *Synechococcus* sp. PCC 7335 (7SA3; tan), and the AlphaFold predictions of FRL-D1 from *C. thermalis* (K9TVY6; plum) and D1 from *P. marinus* MIT 9313 (Q7TTH6; silver). D2 proteins from *Synechocystis* sp. PCC 6803 (white) and *Synechococcus* sp. PCC 7335 (grey) are also shown. Chls (P_{D1} and P_{D2}) and Pheo in the *Synechocystis* sp. PCC 6803 complex are shown in dark and light shades of green, respectively, and those from *Synechococcus* sp. PCC 7335 are shown at 80% transparency.

Our study has revealed that the synthesis of 8V-Chls affects growth, photosystem assembly, and membrane morphology under WL and FRL conditions in the FaRLiP cyanobacterium *C. thermalis*, and details the first biosynthesis of 8V Chls *d* and *f*. Despite 8V reduction being the only dispensable step in the biosynthesis of Chls in oxygenic photoautotrophs, the importance of 8VRs for FaRLiP and growth under high intensity light has been revealed. Future work will focus on characterising the photosynthetic performance of isolated 8V-Chl-containing photosystems assembled under FRL conditions.

bioRxiv preprint doi: https://doi.org/10.1101/2025.05.26.656186; this version posted May 29, 2025. The copyright holder for this preprint (which was not certified by peer review) is the author/funder, who has granted bioRxiv a license to display the preprint in perpetuity. It is made available under a CC-BY 4.0 International license.

AUTHOR CONTRIBUTIONS

AKC, LKF, KP, and GFD data curation; AKC, KP, KP, GFD, DJN, RG and DPC formal analysis; DPC writing–original draft; AKC, LKF, KP, GFD, DJN, and RG writing–review and editing; RG and DPC supervision; DPC funding acquisition.

FUNDING AND ADDITIONAL INFORMATION

This work was supported by grants from the Biotechnology & Biological Sciences Research Council, awards BB/W008076/1 (DPC and LKF) and BB/X015955/1 (DPC). AKC was supported by a University of Liverpool Studentship; DJN by the Deutsche Forschungsgemeinschaft (DFG; Emmy Noether project award no. NU 421/1). The authors gratefully acknowledge the University of Liverpool Biomedical EM Facility for their support and assistance in this work.

DATA AVAILABILTY

The data that support the findings of this study, and materials used herein, are available from the corresponding author upon request.

bioRxiv preprint doi: https://doi.org/10.1101/2025.05.26.656186; this version posted May 29, 2025. The copyright holder for this preprint (which was not certified by peer review) is the author/funder, who has granted bioRxiv a license to display the preprint in perpetuity. It is made available under a CC-BY 4.0 International license.

REFERENCES

1. Bryant DA, Canniffe DP. How nature designs light-harvesting antenna systems: design principles and functional realization in chlorophototrophic prokaryotes. Journal of Physics B: Atomic, Molecular and Optical Physics. 2018 Jan 17;51(3):033001. https://doi.org/10.1088/1361-6455/aa9c3c

2. La Roche J, Van der Staay GW, Partensky F, Ducret A, Aebersold R, Li R, Golden SS, Hiller RG, Wrench PM, Larkum AW, Green BR. Independent evolution of the prochlorophyte and green plant chlorophyll a/b light-harvesting proteins. Proceedings of the National Academy of Sciences. 1996 Dec 24;93(26):15244-8. https://doi.org/10.1073/pnas.93.26.15244

3. Partensky F, Six C, Ratin M, Garczarek L, Vaulot D, Probert I, Calteau A, Gourvil P, Marie D, Grébert T, Bouchier C Le Panse S, Gachenot, M, Rodríguez F, Garrido JL. A novel species of the marine cyanobacterium Acaryochloris with a unique pigment content and lifestyle. Scientific Reports. 2018 Jun 14;8(1):9142. https://doi.org/10.1038/s41598-018-27542-7

4. Kume A, Akitsu T, Nasahara KN. Why is chlorophyll b only used in light-harvesting systems? Journal of Plant research. 2018 Nov;131:961-72. https://doi.org/10.1007/s10265-018-1052-7

5. Miyashita H, Ikemoto H, Kurano N, Adachi K, Chihara M, Miyachi S. Chlorophyll d as a major pigment. Nature. 1996 Oct 3;383(6599):402. https://doi.org/10.1038/383402a0

6. Chen M, Schliep M, Willows RD, Cai ZL, Neilan BA, Scheer H. A red-shifted chlorophyll. Science. 2010 Sep 10;329(5997):1318-9. DOI: 10.1126/science.1191127

7. Chen M, Li Y, Birch D, Willows RD. A cyanobacterium that contains chlorophyll f–a red-absorbing photopigment. FEBS letters. 2012 Sep 21;586(19):3249-54. https://doi.org/10.1016/j.febslet.2012.06.045

8. Gan F, Zhang S, Rockwell NC, Martin SS, Lagarias JC, Bryant DA. Extensive remodeling of a cyanobacterial photosynthetic apparatus in far-red light. Science. 2014 Sep 12;345(6202):1312-7. DOI: 10.1126/science.1256963

9. Gan F, Shen G, Bryant DA. Occurrence of far-red light photoacclimation (FaRLiP) in diverse cyanobacteria. Life. 2014 Dec 29;5(1):4-24. https://doi.org/10.3390/life5010004

bioRxiv preprint doi: https://doi.org/10.1101/2025.05.26.656186; this version posted May 29, 2025. The copyright holder for this preprint (which was not certified by peer review) is the author/funder, who has granted bioRxiv a license to display the preprint in perpetuity. It is made available under a CC-BY 4.0 International license.

10. Antonaru LA, Rad-Menéndez C, Mbedi S, Sparmann S, Pope M, Oliver T, Wu S, Green DH, Gugger M, Nürnberg DJ. Evolution of far-red light photoacclimation in cyanobacteria. Current Biology. 2025 May 13. 10.1016/j.cub.2025.04.038

11. Ho MY, Shen G, Canniffe DP, Zhao C, Bryant DA. Light-dependent chlorophyll f synthase is a highly divergent paralog of PsbA of photosystem II. Science. 2016 Aug 26;353(6302):aaf9178. DOI: 10.1126/science.aaf9178

12. Trinugroho JP, Bečková M, Shao S, Yu J, Zhao Z, Murray JW, Sobotka R, Komenda J, Nixon PJ. Chlorophyll f synthesis by a super-rogue photosystem II complex. Nature Plants. 2020 Mar 13;6(3):238-44. https://doi.org/10.1038/s41477-020-0616-4

13. Chisholm SW, Frankel SL, Goericke R, Olson RJ, Palenik B, Waterbury JB, West-Johnsrud L, Zettler ER. Prochlorococcus marinus nov. gen. nov. sp.: an oxyphototrophic marine prokaryote containing divinyl chlorophyll a and b. Archives of Microbiology. 1992 Feb;157:297-300. https://doi.org/10.1007/BF00245165

14. Nagata N, Tanaka R, Satoh S, Tanaka A. Identification of a vinyl reductase gene for chlorophyll synthesis in Arabidopsis thaliana and implications for the evolution of Prochlorococcus species. The Plant Cell. 2005 Jan;17(1):233-40. https://doi.org/10.1105/tpc.104.027276

15. Nakanishi H, Nozue H, Suzuki K, Kaneko Y, Taguchi G, Hayashida N. Characterization of the Arabidopsis thaliana mutant pcb2 which accumulates divinyl chlorophylls. Plant and cell physiology. 2005 Mar 1;46(3):467-73. https://doi.org/10.1093/pcp/pci053

16. Wang P, Gao J, Wan C, Zhang F, Xu Z, Huang X, Sun X, Deng X. Divinyl chlorophyll (ide) a can be converted to monovinyl chlorophyll (ide) a by a divinyl reductase in rice. Plant physiology. 2010 Jul;153(3):994-1003. https://doi.org/10.1104/pp.110.158477

17. Wang P, Wan C, Xu Z, Wang P, Wang W, Sun C, Ma X, Xiao Y, Zhu J, Gao X, Deng X. One divinyl reductase reduces the 8-vinyl groups in various intermediates of chlorophyll biosynthesis in a given higher plant species, but the isozyme differs between species. Plant physiology. 2013 Jan;161(1):521-34. https://doi.org/10.1104/pp.112.208421

bioRxiv preprint doi: https://doi.org/10.1101/2025.05.26.656186; this version posted May 29, 2025. The copyright holder for this preprint (which was not certified by peer review) is the author/funder, who has granted bioRxiv a license to display the preprint in perpetuity. It is made available under a CC-BY 4.0 International license.

18. Gomez Maqueo Chew A, Bryant DA. Characterization of a plant-like protochlorophyllide a divinyl reductase in green sulfur bacteria. Journal of Biological Chemistry. 2007 Feb 2;282(5):2967-75. https://doi.org/10.1074/jbc.M609730200

19. Canniffe DP, Jackson PJ, Hollingshead S, Dickman MJ, Hunter CN. Identification of an 8-vinyl reductase involved in bacteriochlorophyll biosynthesis in Rhodobacter sphaeroides and evidence for the existence of a third distinct class of the enzyme. Biochemical Journal. 2013 Mar 1;450(2):397-405. https://doi.org/10.1042/BJ20121723

20. Nagata N, Tanaka R, Tanaka A. The major route for chlorophyll synthesis includes [3, 8-divinyl]-chlorophyllide a reduction in Arabidopsis thaliana. Plant and cell physiology. 2007 Dec 1;48(12):1803-8. https://doi.org/10.1093/pcp/pcm153

21. Ito H, Yokono M, Tanaka R, Tanaka A. Identification of a novel vinyl reductase gene essential for the biosynthesis of monovinyl chlorophyll in Synechocystis sp. PCC6803. Journal of Biological Chemistry. 2008 Apr 4;283(14):9002-11. https://doi.org/10.1074/jbc.M708369200

22. Islam MR, Aikawa S, Midorikawa T, Kashino Y, Satoh K, Koike H. slr1923 of Synechocystis sp. PCC6803 is essential for conversion of 3, 8-divinyl (proto) chlorophyll (ide) to 3-monovinyl (proto) chlorophyll(ide). Plant physiology. 2008 Oct;148(2):1068-81. https://doi.org/10.1104/pp.108.123117

23. Liu Z, Bryant DA. Multiple types of 8-vinyl reductases for (bacterio) chlorophyll biosynthesis occur in many green sulfur bacteria. Journal of bacteriology. 2011 Sep 15;193(18):4996-8. https://doi.org/10.1128/JB.05520-11

24. Saunders AH, Golbeck JH, Bryant DA. Characterization of BciB: a ferredoxin-dependent 8-vinyl-protochlorophyllide reductase from the green sulfur bacterium Chloroherpeton thalassium. Biochemistry. 2013 Nov 26;52(47):8442-51. https://doi.org/10.1021/bi401172b

25. Chen GE, Hitchcock A, Jackson PJ, Chaudhuri RR, Dickman MJ, Hunter CN, Canniffe DP. Two unrelated 8-vinyl reductases ensure production of mature chlorophylls in Acaryochloris marina. Journal of Bacteriology. 2016 May 1;198(9):1393-400. https://doi.org/10.1128/jb.00925-15

26. Rippka R, Deruelles J, Waterbury JB, Herdman M, Stanier RY. Generic assignments, strain histories and properties of pure cultures of cyanobacteria. Microbiology. 1979 Mar;111(1):1-61. https://doi.org/10.1099/00221287-111-1-1

bioRxiv preprint doi: https://doi.org/10.1101/2025.05.26.656186; this version posted May 29, 2025. The copyright holder for this preprint (which was not certified by peer review) is the author/funder, who has granted bioRxiv a license to display the preprint in perpetuity. It is made available under a CC-BY 4.0 International license.

27. Cai YP, Wolk CP. Use of a conditionally lethal gene in Anabaena sp. strain PCC 7120 to select for double recombinants and to entrap insertion sequences. Journal of bacteriology. 1990 Jun;172(6):3138-45. https://doi.org/10.1128/jb.172.6.3138-3145.1990

28. Koksharova OA, Wolk CP. A novel gene that bears a DnaJ motif influences cyanobacterial cell division. Journal of Bacteriology. 2002 Oct 1;184(19):5524-8. https://doi.org/10.1128/JB.184.19.5524-5528.2002

29. Elhai J, Vepritskiy A, Muro-Pastor AM, Flores E, Wolk CP. Reduction of conjugal transfer efficiency by three restriction activities of Anabaena sp. strain PCC 7120. Journal of bacteriology. 1997 Mar;179(6):1998-2005. https://doi.org/10.1128/jb.179.6.1998-2005.1997

30. Elhai J, Wolk CP. [83] Conjugal transfer of DNA to cyanobacteria. InMethods in enzymology 1988 Jan 1 (Vol. 167, pp. 747-754). Academic Press. https://doi.org/10.1016/0076-6879(88)67086-8

31. Canniffe DP, Jackson PJ, Hollingshead S, Dickman MJ, Hunter CN. Identification of an 8-vinyl reductase involved in bacteriochlorophyll biosynthesis in Rhodobacter sphaeroides and evidence for the existence of a third distinct class of the enzyme. Biochemical Journal. 2013 Mar 1;450(2):397-405. https://doi.org/10.1042/BJ20121723

32. Li Y, Lin Y, Loughlin PC, Chen M. Optimization and effects of different culture conditions on growth of Halomicronema hongdechloris–a filamentous cyanobacterium containing chlorophyll f. Frontiers in plant science. 2014 Feb 25;5:67. https://doi.org/10.3389/fpls.2014.00067

33. Nürnberg DJ, Morton J, Santabarbara S, Telfer A, Joliot P, Antonaru LA, Ruban AV, Cardona T, Krausz E, Boussac A, Fantuzzi A. Rutherford AW. Photochemistry beyond the red limit in chlorophyll f–containing photosystems. Science. 2018 Jun 15;360(6394):1210-3. DOI: 10.1126/science.aar8313

34. MacGregor-Chatwin C, Nürnberg DJ, Jackson PJ, Vasilev C, Hitchcock A, Ho MY, Shen G, Gisriel CJ, Wood WH, Mahbub M, Selinger VM, Johnson MP, Dickman MJ, Rutherford AW, Brant DA, Hunter CN. Changes in supramolecular organization of cyanobacterial thylakoid membrane complexes in response to far-red light photoacclimation. Science advances. 2022 Feb 9;8(6):eabj4437. DOI: 10.1126/sciadv.abj4437

35. Chen J, Kell A, Acharya K, Kupitz C, Fromme P, Jankowiak R. Critical assessment of the emission spectra of various photosystem II core complexes. Photosynthesis Research. 2015 Jun;124:253-65. https://doi.org/10.1007/s11120-015-0128-7

bioRxiv preprint doi: https://doi.org/10.1101/2025.05.26.656186; this version posted May 29, 2025. The copyright holder for this preprint (which was not certified by peer review) is the author/funder, who has granted bioRxiv a license to display the preprint in perpetuity. It is made available under a CC-BY 4.0 International license.

36. Heinz S, Rast A, Shao L, Gutu A, Gügel IL, Heyno E, Labs M, Rengstl B, Viola S, Nowaczyk MM, Leister D, Nickelsen J. Thylakoid membrane architecture in Synechocystis depends on CurT, a homolog of the granal CURVATURE THYLAKOID1 proteins. The Plant Cell. 2016 Sep 1;28(9):2238-60. https://doi.org/10.1105/tpc.16.00491

37. Armbruster U, Labs M, Pribil M, Viola S, Xu W, Scharfenberg M, Hertle AP, Rojahn U, Jensen PE, Rappaport F, Joliot P, Dörmann P, Wanner G, Leister D. Arabidopsis CURVATURE THYLAKOID1 proteins modify thylakoid architecture by inducing membrane curvature. The Plant Cell. 2013 Jul 1;25(7):2661-78. https://doi.org/10.1105/tpc.113.113118

38. Zhen S, van Iersel MW, Bugbee B. Photosynthesis in sun and shade: the surprising importance of far-red photons. New Phytologist. 2022 Oct;236(2):538-46. https://doi.org/10.1111/nph.18375

39. Caiola MG, Billi D. Chroococcidiopsis from desert to mars. InAlgae and cyanobacteria in extreme environments 2007 (pp. 553-568). Dordrecht: Springer Netherlands. https://doi.org/10.1007/978-1-4020-6112-7_30

40. Airs RL, Temperton B, Sambles C, Farnham G, Skill SC, Llewellyn CA. Chlorophyll f and chlorophyll d are produced in the cyanobacterium Chlorogloeopsis fritschii when cultured under natural light and near-infrared radiation. Febs Letters. 2014 Oct 16;588(20):3770-7. https://doi.org/10.1016/j.febslet.2014.08.026

41. Sim MS, Liang B, Petroff AP, Evans A, Klepac-Ceraj V, Flannery DT, Walter MR, Bosak T. Oxygen-dependent morphogenesis of modern clumped photosynthetic mats and implications for the Archean stromatolite record. Geosciences. 2012 Oct 11;2(4):235-59. https://doi.org/10.3390/geosciences2040235

42. Hernández-Prieto MA, Li Y, Postier BL, Blankenship RE, Chen M. Far-red light promotes biofilm formation in the cyanobacterium Acaryochloris marina. Environmental Microbiology. 2018 Feb;20(2):535-45. https://doi.org/10.1111/1462-2920.13961

43. Mella-Flores D, Six C, Ratin M, Partensky F, Boutte C, Le Corguillé G, Marie D, Blot N, Gourvil P, Kolowrat C, Garczarek L. Prochlorococcus and Synechococcus have evolved different adaptive mechanisms to cope with light and UV stress. Frontiers in microbiology. 2012 Aug 8;3:285. https://doi.org/10.3389/fmicb.2012.00285

bioRxiv preprint doi: https://doi.org/10.1101/2025.05.26.656186; this version posted May 29, 2025. The copyright holder for this preprint (which was not certified by peer review) is the author/funder, who has granted bioRxiv a license to display the preprint in perpetuity. It is made available under a CC-BY 4.0 International license.

586 44. Ito H, Tanaka A. Evolution of a divinyl chlorophyll-based photosystem in Prochlorococcus. Proceedings of
587 the National Academy of Sciences. 2011 Nov 1;108(44):18014-9.
588 https://doi.org/10.1073/pnas.1107590108
589
590 45. Gisriel CJ, Wang J, Liu J, Flesher DA, Reiss KM, Huang HL, Yang KR, Armstrong WH, Gunner MR, Batista
591 VS, Debus RJ, Brudvig GW. High-resolution cryo-electron microscopy structure of photosystem II from
592 the mesophilic cyanobacterium, Synechocystis sp. PCC 6803. Proceedings of the National Academy of
593 Sciences. 2022 Jan 4;119(1):e2116765118. https://doi.org/10.1073/pnas.2116765118
594
595 46. Gisriel CJ, Shen G, Ho MY, Kurashov V, Flesher DA, Wang J, Armstrong WH, Golbeck JH, Gunner MR,
596 Vinyard DJ, Debus RJ, Brudvig GW, Bryant DA. Structure of a monomeric photosystem II core complex
597 from a cyanobacterium acclimated to far-red light reveals the functions of chlorophylls d and f. Journal
598 of Biological Chemistry. 2022 Jan 1;298(1). 10.1016/j.jbc.2021.101424
599
600 47. Varadi M, Bertoni D, Magana P, Paramval U, Pidruchna I, Radhakrishnan M, Tsenkov M, Nair S, Mirdita
601 M, Yeo J, Kovalevskiy O, Tunyasuvunakool K, Laydon A, Žídek A, Tomlinson H, Hariharan D, Abrahamson
602 J, Green T, Jumper J, Birney E, Steinegger M, Hassabis D, Velankar S. AlphaFold Protein Structure
603 Database in 2024: providing structure coverage for over 214 million protein sequences. Nucleic acids
604 research. 2024 Jan 5;52(D1):D368-75. https://doi.org/10.1093/nar/gkad1011